Supplementary Material for

Quantifying the contributions of atmospheric processes and meteorology to severe $PM_{2.5}$ pollution episodes during the COVID-19 lockdown in the Beijing-Tianjin-Hebei, China

Ishaq Dimeji Sulaymon[a], Yuanxun Zhang[b,c], Philip K. Hopke[d,e], Song Guo[f], Fei Ye[a], Jinjin Sun[a], Yanhong Zhu[a], Jianlin Hu[a*]

[a] *Jiangsu Key Laboratory of Atmospheric Environment Monitoring and Pollution Control, Collaborative Innovation Center of Atmospheric Environment and Equipment Technology, School of Environmental Science and Engineering, Nanjing University of Information Science and Technology, Nanjing, 210044, China*

[b] *College of Resources and Environment, University of Chinese Academy of Sciences, Beijing 100049, China*

[c] *CAS Center for Excellence in Regional Atmospheric Environment, Chinese Academy of Sciences, Xiamen, 361021, China*

[d] *Center for Air Resources Engineering and Science, Clarkson University, Potsdam, NY 13699, USA*

[e] *Department of Public Health Sciences, University of Rochester School of Medicine and Dentistry, Rochester, NY 14642, USA*

[f] *State Key Joint Laboratory of Environmental Simulation and Pollution Control, College of Environmental Sciences and Engineering, Peking University, Beijing, 100871, China*

---

[*] Corresponding author. *E-mail address:* sulaymondimeji@nuist.edu.cn; jianlinhu@nuist.edu.cn

Text S1. Materials and methods

To evaluate the effects of the reduction in anthropogenic emissions sectors on air quality, two scenarios were simulated for comparison (Table S2). For the base case scenario (Case 1), the original anthropogenic emission inventory of the Multi-resolution Emission Inventory for China based on year 2016 (MEIC16) was used. In scenario 2 (Case 2), the industrial, transportation, and power emissions sectors were scaled with a factor of 0.80 (20% reduction), 0.20 (80% reduction), and 0.90 (10% reduction), respectively. The transportation sector was greatly reduced (80%) as both public and private transport systems except those rendering essential services (such as security operatives and hospital vehicles) were shut down nationwide during the lockdown period. The industrial sector was only reduced by 20% as industries producing essential items (such as food, toiletries, face mask, drugs, and so on) were allowed to operate (though not at full scale) during the lockdown period. The emissions from power plants were reduced by 10% in Case 2 due to the closure of offices, schools, restaurants, business centers, non-essential industries, shopping malls, and other public outlets that were also consumers of electricity aside the residential usage. In addition, since the lockdown period coincided with the winter period, the demand for and consumption of power for home heating as well as lighting became highly necessary, hence, no substantive reduction (>10%) in power sector could be justified during the lockdown. The emissions from residential sector were held constant in Case 2 (similar to Case1) since people were mandated to stay at home as a physical way of curtailing the spread of the pandemic. In the absence of official emission inventory during the lockdown, the emission scaling factors used in this study followed the suggestions by the Chinese Research Academy of Environmental Sciences (CRAES 2020) regarding the

status of emission inventory in China during the lockdown and were also consistent with those of Sulaymon et al. (2021a) and Wang et al. (2020).

Text S2. Diel variations of atmospheric processes contributing to $PM_{2.5}$ at the surface layer

The diel variations for the contributions of individual atmospheric processes to the formation of $PM_{2.5}$ and the hourly variations of $PM_{2.5}$ concentrations at the surface layer for the two cases are presented in Fig. S4. Considering Case 2, the positive contributions of EMIS process exhibited two slight increasing trends during 05:00 local time (LT) to 07:00 LT and 15:00-20:00 LT in BTH, Beijing, Shijiazhuang, and Baoding, while it only showed a small increasing trend in Tianjin during 15:00-20:00 LT. EMIS process displayed a bimodal feature in BTH, Beijing, Shijiazhuang, and Baoding at 07:00 LT and 20:00 LT. Also, the positive contributions due to AERO process showed two increasing trends in BTH (04:00-08:00 LT and 15:00-20:00 LT), Beijing (04:00-07:00 LT and 15:00-19:00 LT), Tianjin (04:00-07:00 LT and 16:00-20:00 LT), Shijiazhuang (04:00-08:00 LT and 15:00-20:00 LT), and Baoding (03:00-07:00 LT and 15:00-20:00 LT). AERO process exhibited two peaks in Tianjin and Baoding (07:00 LT and 20:00 LT), BTH and Shijiazhuang (08:00 LT and 20:00 LT), and Beijing (07:00 LT and 19:00 LT). The first peak of $PM_{2.5}$ concentration occurred at 07:00 LT (in Beijing and Tianjin) and 08:00 LT (in BTH region, Shijiazhuang, and Baoding). During the first periods of increasing trends of EMIS and AERO in Beijing and Tianjin, both HTRA and VTRA were the major sinks, resulting into vertical and horizontal exports of $PM_{2.5}$ in the two cities. Contrarily, in BTH, Shijiazhuang, and Baoding, HTRA, just like EMIS and AERO, also contributed positively to the net

$PM_{2.5}$, especially during the nighttime and early hours of the day, while VTRA served as the predominant sink, resulting into horizontal import and vertical export of $PM_{2.5}$. During the nighttime and early hours of the day, the contributions of HTRA were the dominant $PM_{2.5}$ import in Shijiazhuang, with the two peaks occurring at 00:00 LT and 21:00 LT. However, HTRA changed from positive to negative in BTH (11:00-15:00 LT), Shijiazhuang (10:00-17:00 LT), and Baoding (09:00-16:00 LT) and acted as another sink. It is worthy to note that during 13:00-1600 LT and 14:00-1500 LT in Shijiazhuang and Baoding, respectively, the contributions of VTRA became positive, resulting into vertical import and horizontal export of $PM_{2.5}$. The positive effects of EMIS (07:00-15:00 LT in Beijing; 07:00-11:00 LT in Shijiazhuang, Baoding, and BTH) and AERO (07:00-14:00 LT in Beijing; 08:00-12:00 LT in Shijiazhuang; 07:00-15:00 LT in Baoding; and 08:00-15:00 LT in BTH) became weakened and their contributions decreased during the periods. Therefore, the net effects of these positive processes (EMIS and AERO) were insufficient to offset the continuous negative effects of VTRA on $PM_{2.5}$ concentrations, leading to downward trends in $PM_{2.5}$ across the study areas during the periods. It should also be noted that the HTRA effects changed from negative to positive in BTH (16:00-23:00 LT), Beijing (18:00-22:00 LT), Tianjin (15:00-20:00 LT), Shijiazhuang (18:00-23:00 LT), and Baoding (17:00-23:00 LT) and served as another contributor to the net $PM_{2.5}$. As a result of the positive contributions of the EMIS, AERO, and HTRA processes during the nighttime, the already flattened $PM_{2.5}$ levels began to rise again, and the second $PM_{2.5}$ peak occurred at 21:00 LT (in BTH, Beijing, Tianjin, and Shijiazhuang) and 22:00 LT in Baoding. Generally, the EMIS process was the vital source of hourly $PM_{2.5}$ concentrations at the surface, with the highest contributions in BTH region (25.3 $\mu g/m^3/h$ in daytime; 34.4 $\mu g/m^3/h$ in

nighttime), Beijing (43.6 μg/m^3/h in daytime; 55.7 μg/m^3/h in nighttime), Tianjin (53.2 μg/m^3/h in daytime; 76.2 μg/m^3/h in nighttime), and Baoding (36.9 μg/m^3/h in daytime; 48.4 μg/m^3/h in nighttime), while HTRA was the dominant source in Shijiazhuang (37.4 μg/m^3/h in daytime; 48.4 μg/m^3/h in nighttime). Contrarily, $PM_{2.5}$ was substantially removed from the surface layer and transported to the upper layers through the VTRA process, especially during nighttime, with the maximum removal rates of 67.4 μg/m^3/h (21:00 LT), 89.7 μg/m^3/h (20:00 LT), 94.4 μg/m^3/h (20:00 LT), 85.6 μg/m^3/h (21:00 LT), and 94.7 μg/m^3/h (21:00 LT) in BTH region, Beijing, Tianjin, Shijiazhuang, and Baoding, respectively. DDEP and CHEM processes had slight contributions and served as the sink and source of $PM_{2.5}$, respectively. It is worthy to note that the trends of the atmospheric processes and $PM_{2.5}$ in Case 1 were similar to in Case 2 in each of the study areas, however, the contributions of the individual processes to the net $PM_{2.5}$ and the resultant magnitudes of $PM_{2.5}$ changes were higher in Case 1 than Case 2. This was due to the effects of emissions reductions implemented in Case 2.

Text S3. Diel variations of atmospheric processes contributing to $PM_{2.5}$ in the PBL

As illustrated in Fig. S5, the trends of hourly contributions of individual atmospheric processes to the formation of $PM_{2.5}$ as well as the diel distributions of $PM_{2.5}$ concentrations in the PBL were similar to that of surface layer except that the magnitudes were low in PBL relative to the surface layer. Similar to the surface layer, the EMIS process was the major source of $PM_{2.5}$ concentrations in the PBL, with the maximum contributions in BTH region (14.9 μg/m^3/h in daytime; 14.7 μg/m^3/h in nighttime), Beijing (19.6 μg/m^3/h in daytime; 19.1 μg/m^3/h in nighttime), Tianjin (27.1 μg/m^3/h in daytime; 29.6 μg/m^3/h in nighttime), and Baoding (32.4 μg/m^3/h in daytime; 26.9 μg/m^3/h in nighttime), while

HTRA was the dominant $PM_{2.5}$ import in Shijiazhuang (30.2 μg/m^3/h in daytime; 41.0 μg/m^3/h in nighttime). Vertical transport (VTRA) was the major $PM_{2.5}$ removal pathway during most hours of the day except for some hours during the daytime, with the highest removal rates of 32.6 μg/m^3/h, 33.2 μg/m^3/h, 30.8 μg/m^3/h, 55.1 μg/m^3/h, and 60.1 μg/m^3/h in BTH region, Beijing, Tianjin, Shijiazhuang, and Baoding, respectively. Contrary to the surface layer, whose highest VTRA removal rates occurred at the nighttime in all of the study areas, the highest VTRA removal rates in Tianjin and BTH region occurred at 08:00 LT, while that of Baoding occurred at 07:00 LT. Although, the positive contributions of EMIS, AERO, and HTRA pathways to $PM_{2.5}$ formation were low in the PBL relative to the surface layer, however, high $PM_{2.5}$ concentrations were still obtained across the study areas. This could be primarily explained by the low VTRA exports from the PBL compared to the surface layer, resulting to the accumulation of $PM_{2.5}$ within the PBL.

Table S1. The major physics options and the schemes used in the WRF model.

Physics option	Scheme
Microphysics	Thompson scheme
Shortwave radiation	RRTMG scheme
Longwave radiation	RRTMG scheme
Surface layer	Revised MM5 Monin-Obukhov scheme
Land surface	Unified Noah land-surface scheme
Planetary boundary layer	YSU scheme
Cumulus parameterization	Grell-Freitas ensemble scheme

Table S2. Emission scaling factors and the configuration of simulation scenarios

Source sectors	Case 1	Case 2
Residential	No changes	No changes
Industry	No changes	20% reduction
Transportation	No changes	80% reduction
Power	No changes	10% reduction
Agriculture	No changes	No changes

Table S3. Model performance of meteorological factors during the COVID-19 lockdown (OBS: observed mean; PRE: predicted mean; MB: mean bias; ME: mean error; RMSE: root mean square error). The values that do not meet the criteria are highlighted in bold.

		BTH	Beijing	Tianjin	Shijiazhuang	Baoding	Benchmark[a]
T2 (K)	OBS	274.2	273.7	275.1	277.0	274.9	
	PRE	274.6	275.9	275.6	277.6	276.2	
	MB	0.4	**2.2**	0.5	**0.6**	**1.3**	≤±0.5
	ME	1.7	**2.3**	1.1	1.3	1.9	≤2.0
	RMSE	2.1	2.7	1.4	1.6	2.2	
RH (%)	OBS	63.9	63.7	67.5	65.9	68.4	
	PRE	47.5	41.1	49.1	42.9	44.0	
	MB	-16.4	-22.5	-18.4	-23.0	-24.4	
	ME	18.2	22.5	18.4	23.0	24.4	
	RMSE	20.6	24.7	20.3	24.1	26.4	
WS (m/s)	OBS	2.2	2.3	2.3	2.2	1.8	
	PRE	2.7	2.4	2.7	2.9	2.3	
	MB	0.5	0.2	0.4	**0.7**	0.5	≤±0.5
	ME	0.9	0.6	0.6	0.8	0.7	≤2.0
	RMSE	1.2	0.7	0.8	1.1	0.9	≤2.0
WD (°)	OBS	181.6	172.6	195.4	190.7	130.3	
	PRE	172.0	151.7	166.7	192.9	129.5	
	MB	-9.6	**-20.9**	**-28.7**	2.3	-0.8	≤±10
	ME	**70.5**	**78.4**	**45.2**	**101.5**	**50.0**	≤±30
	RMSE	96.9	108.8	69.7	119.8	80.3	

a. The benchmarks used were suggested by Emery et al. (2001).

Table S4. Model performance of $PM_{2.5}$ during the COVID-19 lockdown for the two cases (OBS: observed average; PRE: predicted average; MFB: mean fractional bias; MFE: mean fractional error; MNB: mean normalized bias; MNE: mean normalized error). The performance criteria for $PM_{2.5}$ were suggested by Boylan and Russell (2006).

		BTH	Beijing	Tianjin	Shijiazhuang	Baoding	Benchmark
Case 1							
$PM_{2.5}$ ($\mu g/m^3$)	OBS	73.40	75.13	75.81	98.87	106.85	
	PRE	74.75	81.35	93.14	86.04	102.87	
	MFB	0.10	0.31	0.41	-0.05	-0.19	$\leq \pm 0.60$
	MFE	0.50	0.51	0.51	0.40	0.50	≤ 0.75
	MNB	0.41	0.77	0.91	0.08	0.55	
	MNE	0.70	0.94	0.99	0.43	0.79	
Case 2							
$PM_{2.5}$ ($\mu g/m^3$)	OBS	73.40	75.13	75.81	98.87	106.85	
	PRE	68.99	72.53	83.98	79.20	96.42	
	MFB	-0.03	-0.20	0.32	-0.13	-0.13	$\leq \pm 0.60$
	MFE	0.49	0.50	0.48	0.41	0.49	≤ 0.75
	MNB	0.30	0.56	0.72	-0.01	0.43	
	MNE	0.64	0.80	0.85	0.41	0.72	

Table S5. Averaged predicted $PM_{2.5}$ concentrations of the three pollution episodes (EPs) for Case 2 during COVID-19 lockdown in the BTH region.

Pollution Episodes	EP1	EP2	EP3
City	$PM_{2.5}$ ($\mu g/m^3$)	$PM_{2.5}$ ($\mu g/m^3$)	$PM_{2.5}$ ($\mu g/m^3$)
Beijing	82.8	100.5	77.9
Tianjin	91.7	129.7	92.2
Shijiazhuang	125.1	83.2	66.6
Baoding	133.4	120.4	94.4
Cangzhou	75.0	92.8	79.1
Tangshan	103.6	138.8	98.2
Langfang	85.4	124.6	94.5
Handan	103.6	84.2	68.8
Hengshui	88.6	88.9	82.8
Xingtai	91.7	80.0	60.1

Table S6. Maximum hourly $PM_{2.5}$ concentrations of the three pollution episodes (EPs) for Case 2 during COVID-19 lockdown in the BTH region.

Pollution Episodes	EP1	EP2	EP3
City	$PM_{2.5}$ ($\mu g/m^3$)	$PM_{2.5}$ ($\mu g/m^3$)	$PM_{2.5}$ ($\mu g/m^3$)
Beijing	175.8	200.8	179.0
Tianjin	207.9	233.6	193.6
Shijiazhuang	235.5	222.7	132.0
Baoding	333.1	258.0	187.1
Cangzhou	165.8	178.4	168.0
Tangshan	308.0	308.8	279.1
Langfang	191.6	285.4	211.9
Handan	219.2	165.4	132.4
Hengshui	227.4	163.8	178.4
Xingtai	183.8	186.4	114.1

Table S7. Averaged predicted PBLH and wind speed during the three pollution episodes (EPs) in the four cities.

	PBLH (m)			Wind Speed (m)		
City	EP1	EP2	EP3	EP1	EP2	EP3
Beijing	356.9	255.1	636.5	1.69	1.61	2.33
Tianjin	366.9	262.2	471.7	1.84	1.76	2.42
Shijiazhuang	294.2	341.1	650.6	1.87	2.96	3.63
Baoding	286.9	238.5	517.1	1.79	1.67	2.87

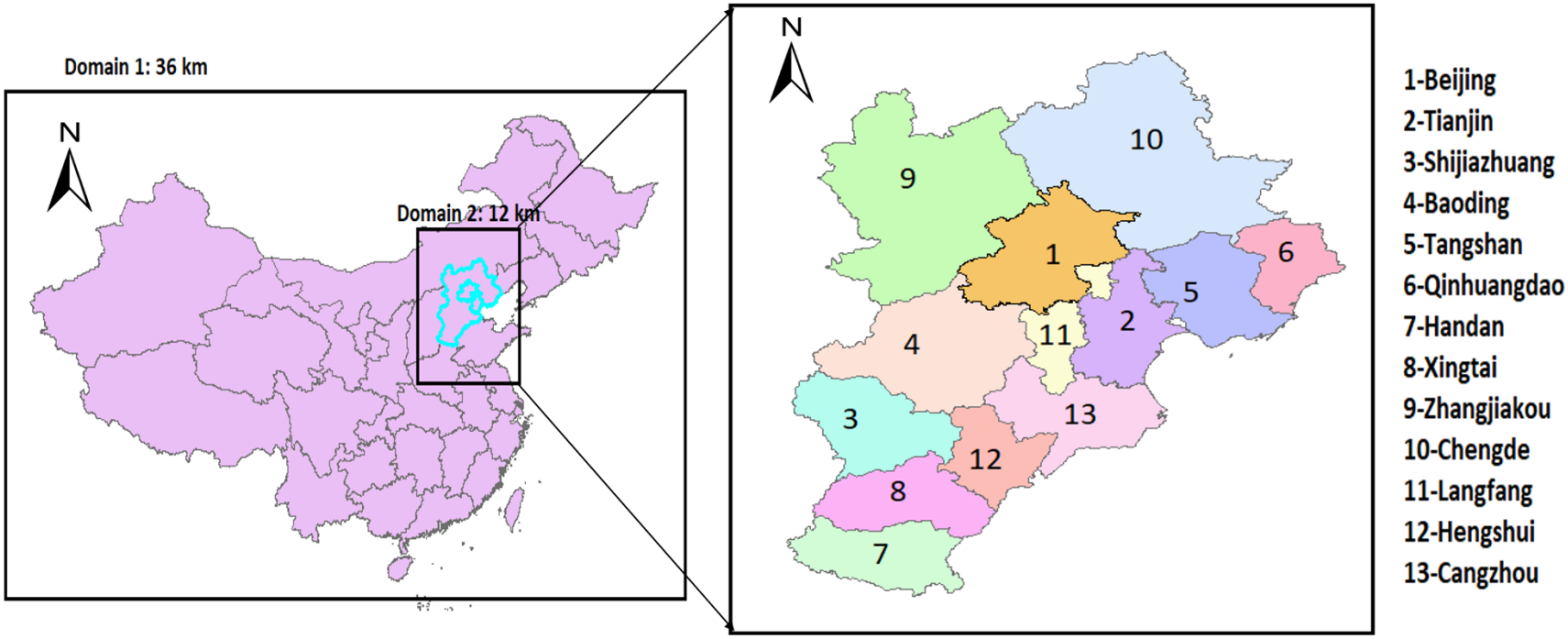

Figure S1. The simulation domains used in this study (left) and the Beijing-Tianjin-Hebei (BTH) region (right). The representative cities were numbered 1-4.

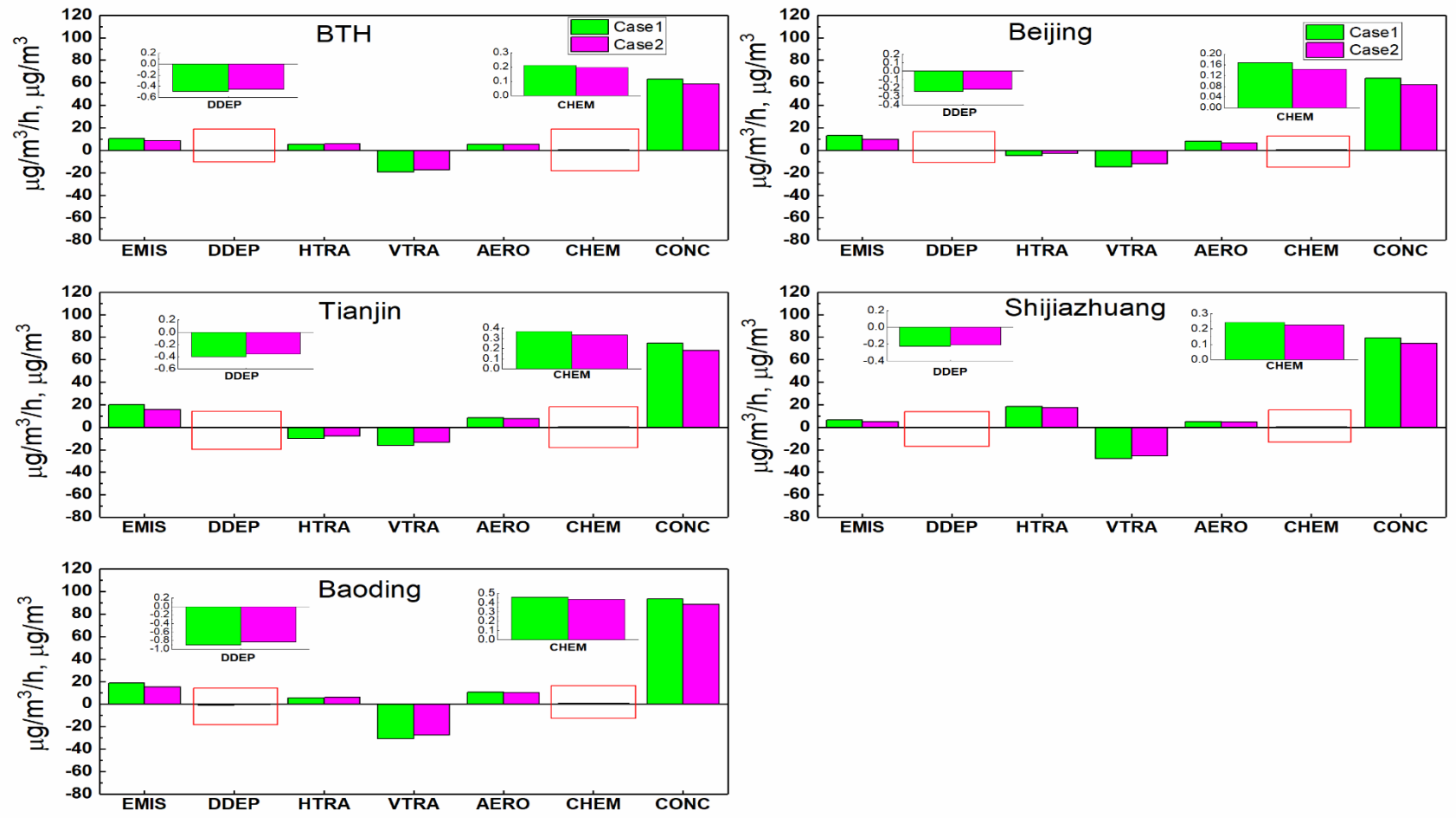

Figure S2. Contributions of the individual processes to the concentrations of $PM_{2.5}$ in the planetary boundary layer (PBL) in Cases 1 and 2 during the lockdown period. Abbreviations used in this figure are the same as in Fig. 1.

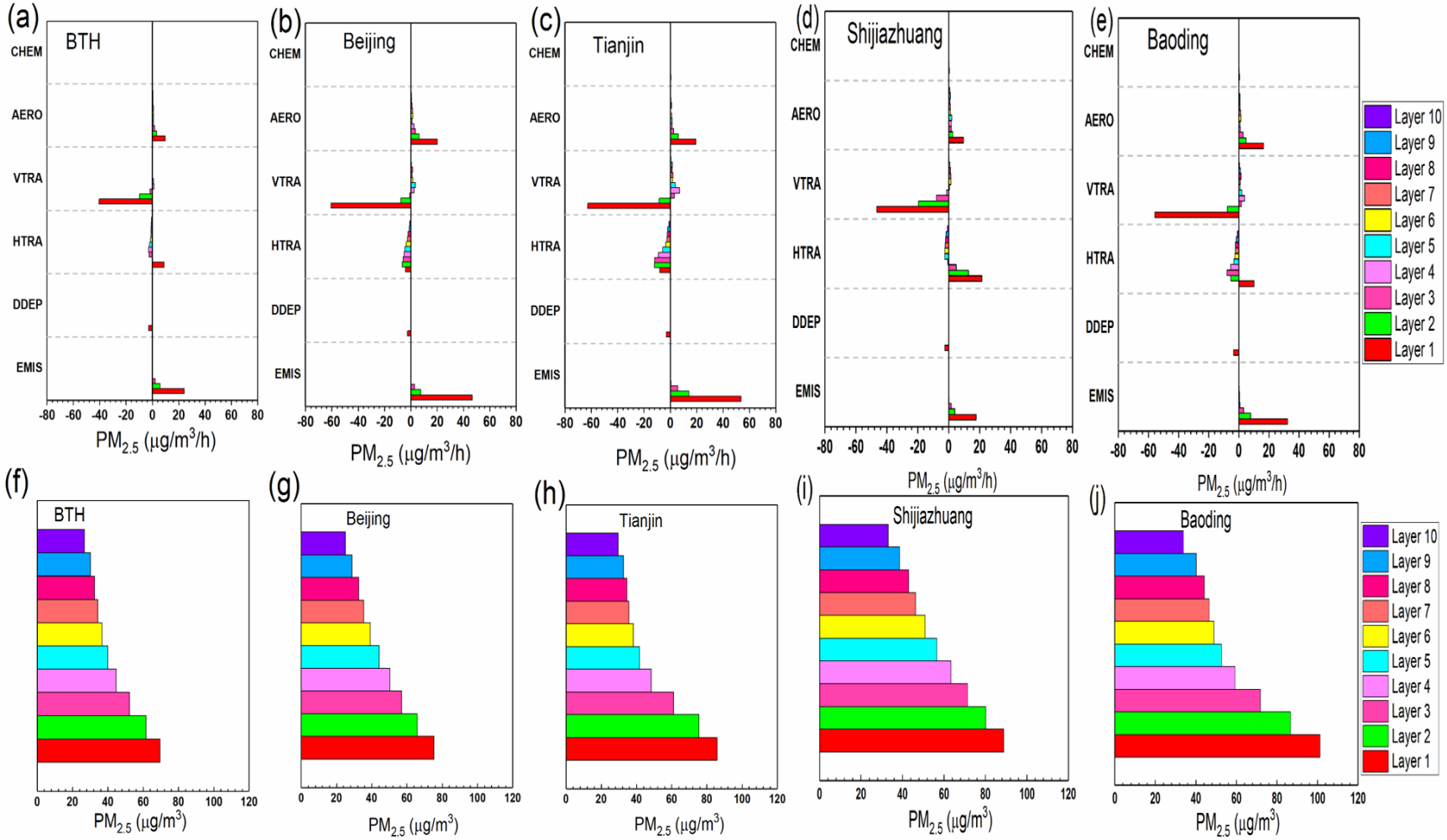

Figure S3. Hourly $PM_{2.5}$ change rates due to individual atmospheric processes for layers 1-10 (a-e) and evolution of hourly $PM_{2.5}$ vertical profiles (f-j) in Case 1 during the lockdown period. Abbreviations used in this figure are the same as in Fig. 1.

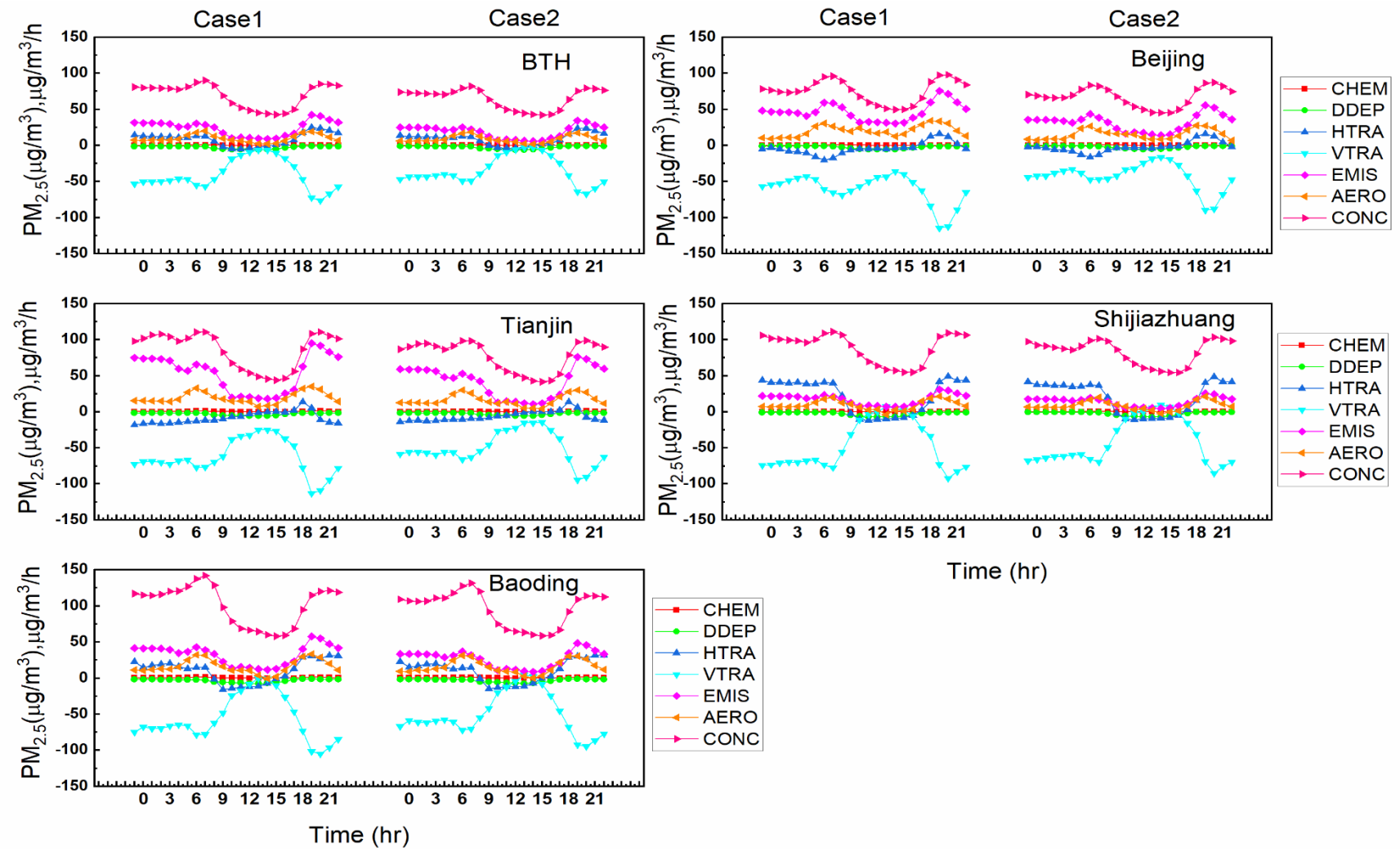

Figure S4. Diel variations of contributions of individual processes to $PM_{2.5}$ formation at the surface layer in Cases 1 and 2 during the lockdown period. Abbreviations used in this figure are the same as in Fig. 1.

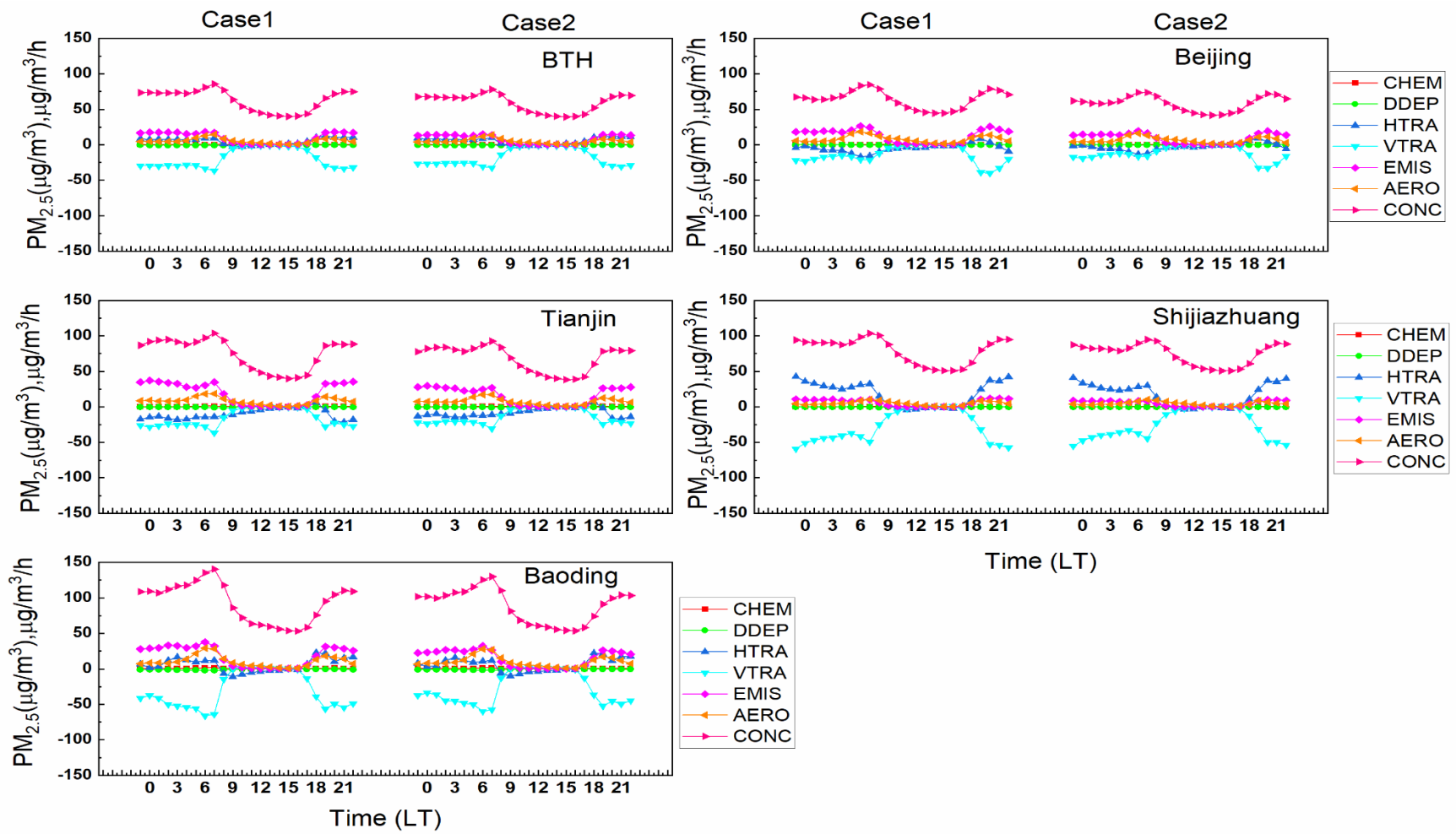

Figure S5. Diel variations of contributions of individual processes to $PM_{2.5}$ formation in the planetary boundary layer (PBL) in Cases 1 and 2 during the lockdown period. Abbreviations used in this figure are the same as in Fig. 1.

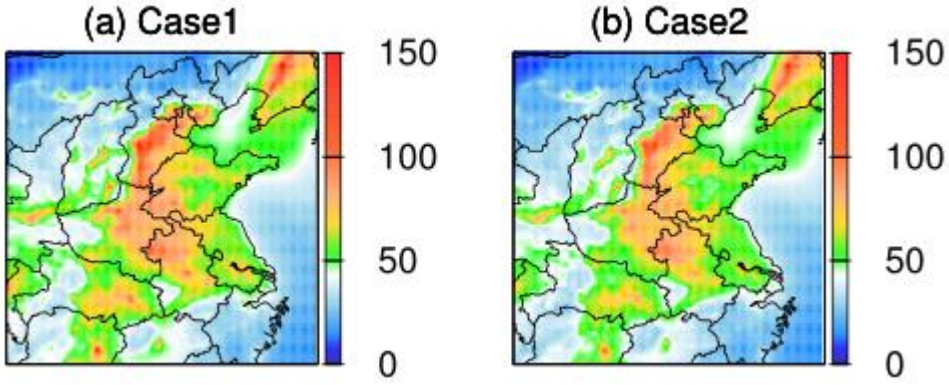

Figure S6. Spatial distributions of predicted $PM_{2.5}$ during lockdown (a) Case1 and (b) Case2 in the BTH region. Units are $\mu g/m^3$.

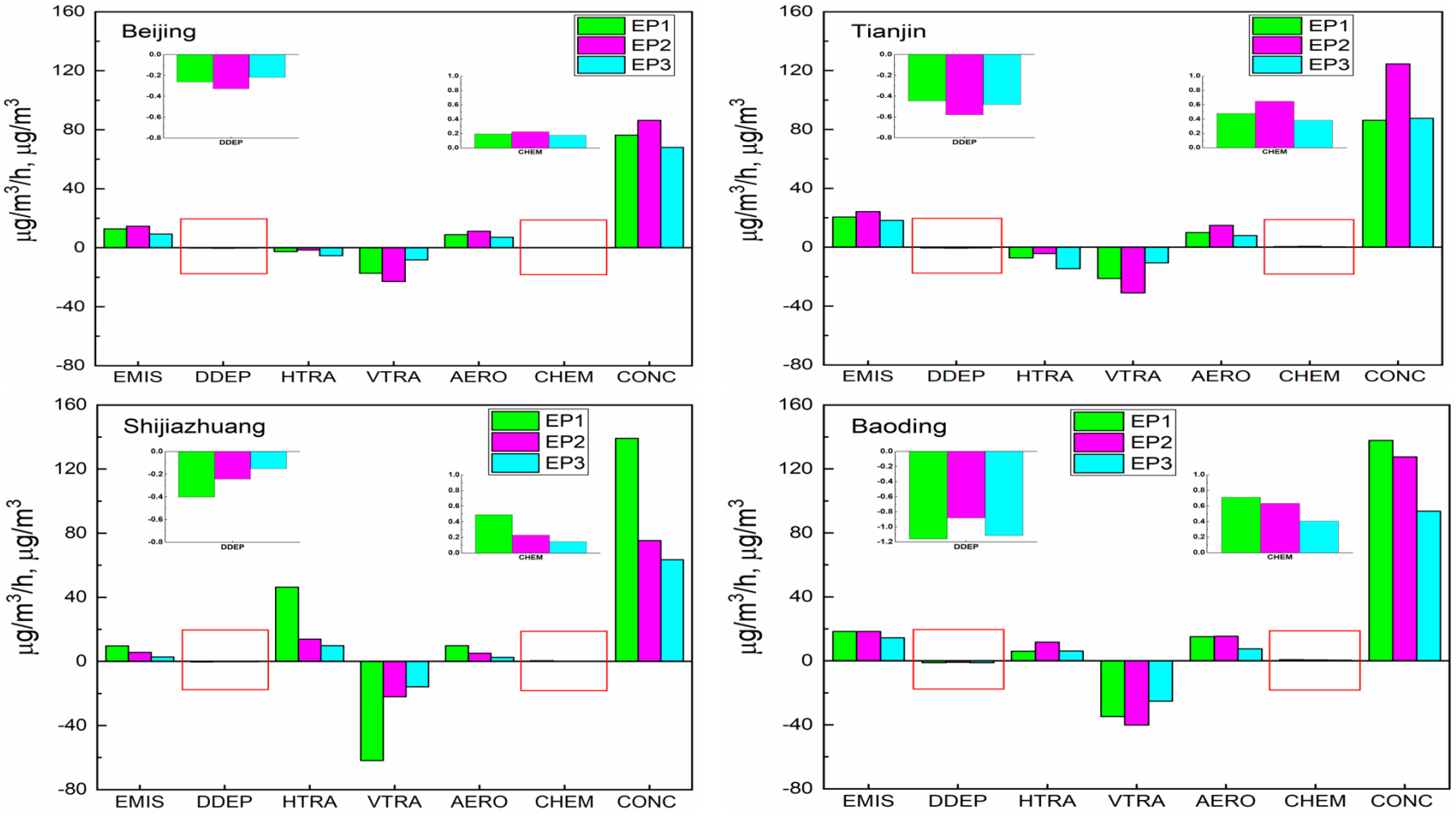

Figure S7. Contributions of the individual processes to the concentrations of $PM_{2.5}$ (Case 2) in the PBL during the three pollution episodes in the four representative cities. Abbreviations used in this figure are the same as in Fig. 1.

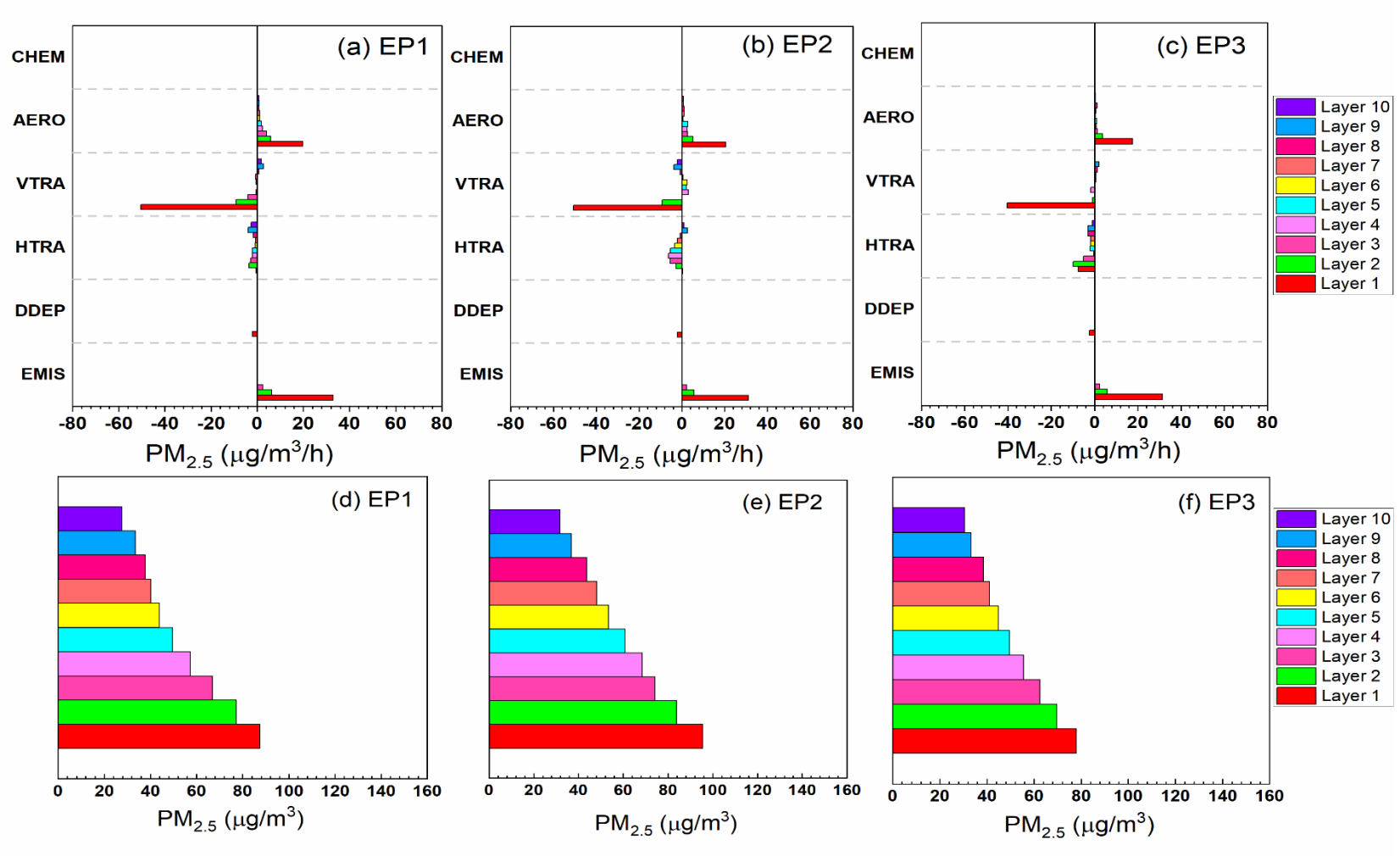

Figure S8. Hourly $PM_{2.5}$ change rates (Case 2) due to individual atmospheric processes for layers 1-10 (a-c) and evolution of hourly $PM_{2.5}$ vertical profiles (d-f) during the three pollution episodes in Beijing. Abbreviations used in this figure are the same as in Fig. 1.

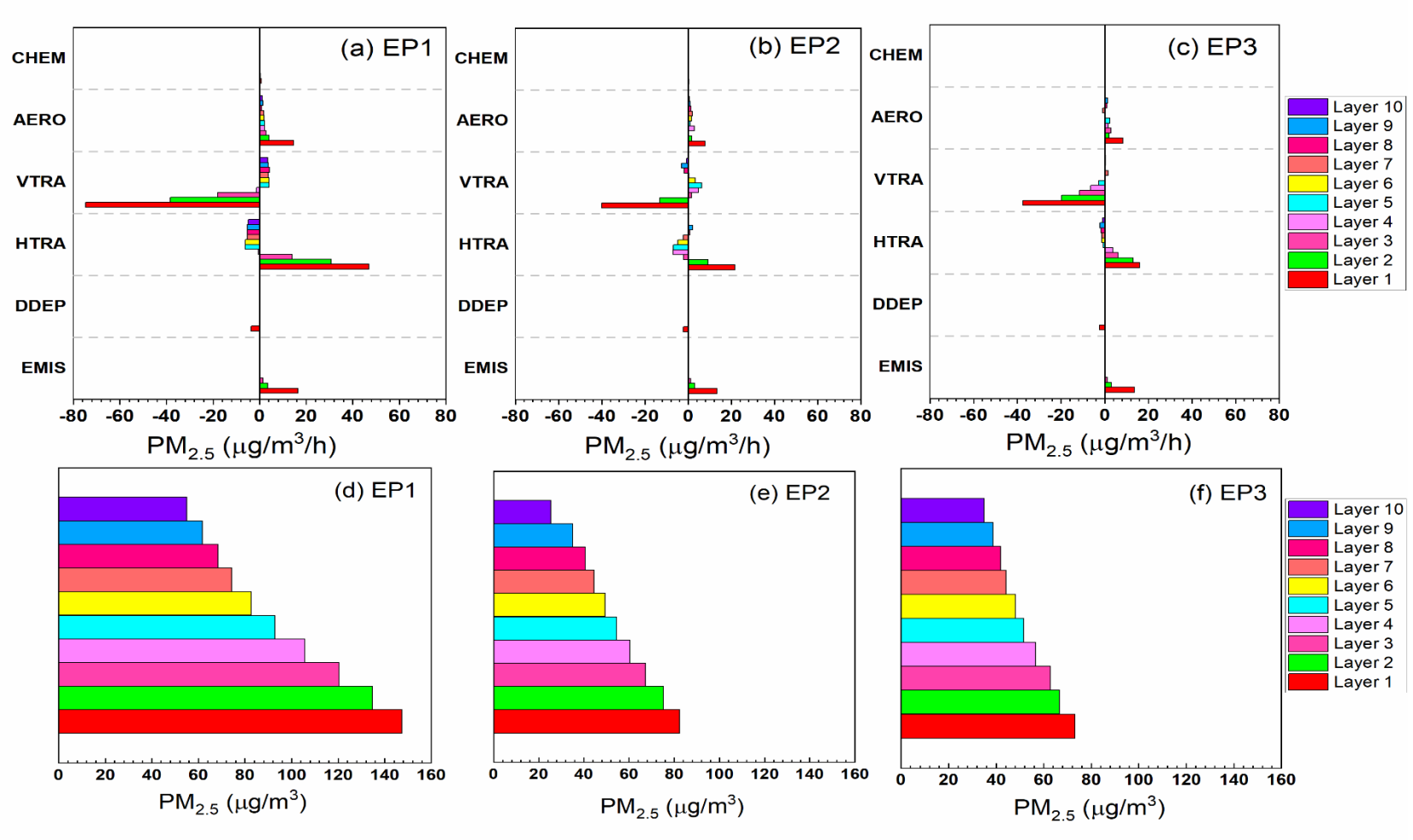

Figure S9. Hourly $PM_{2.5}$ change rates (Case 2) due to individual atmospheric processes for layers 1-10 (a-c) and evolution of hourly $PM_{2.5}$ vertical profiles (d-f) during the three pollution episodes in Shijiazhuang. Abbreviations used in this figure are the same as in Fig. 1.

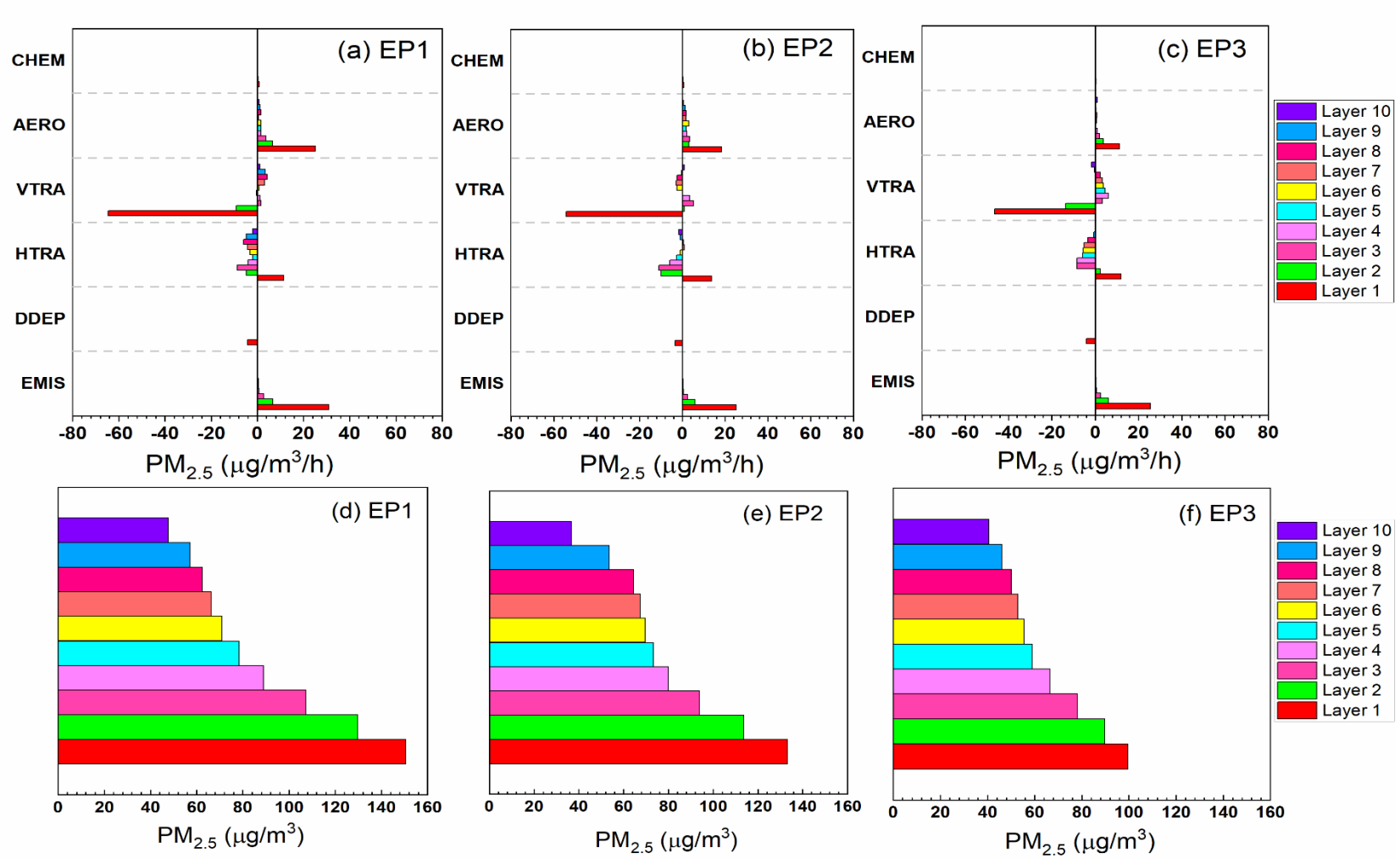

Figure S10. Hourly $PM_{2.5}$ change rates (Case 2) due to individual atmospheric processes for layers 1-10 (a-c) and evolution of hourly $PM_{2.5}$ vertical profiles (d-f) during the three pollution episodes in Baoding. Abbreviations used in this figure are the same as in Fig. 1.

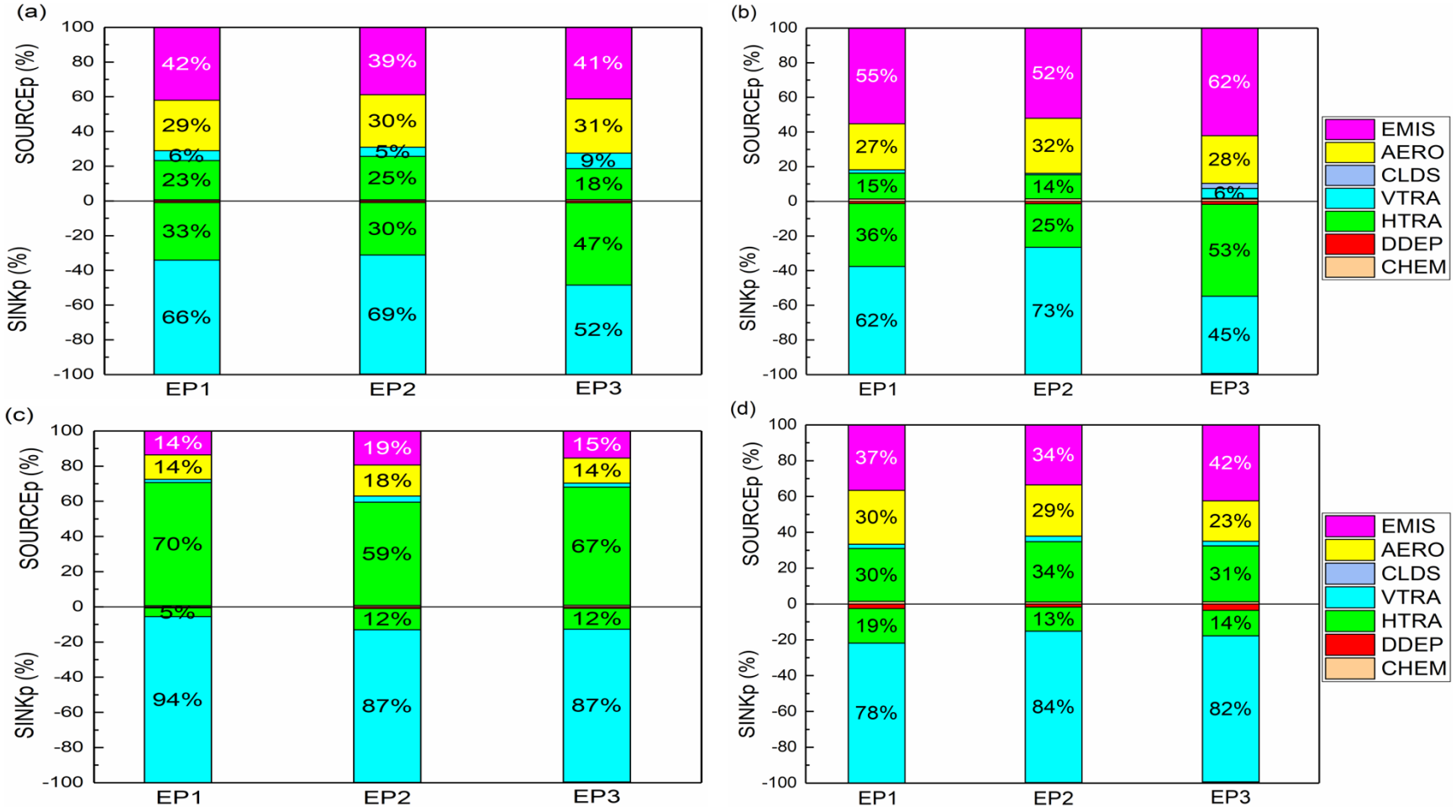

Figure S11. Positive and negative contribution ratios of the individual processes to $PM_{2.5}$ concentrations (Case 2) in the PBL in (a) Beijing, (b) Tianjin, (c) Shijiazhuang, and (d) Baoding during the three pollution episodes. Abbreviations used in this figure are the same as in Fig. 2.

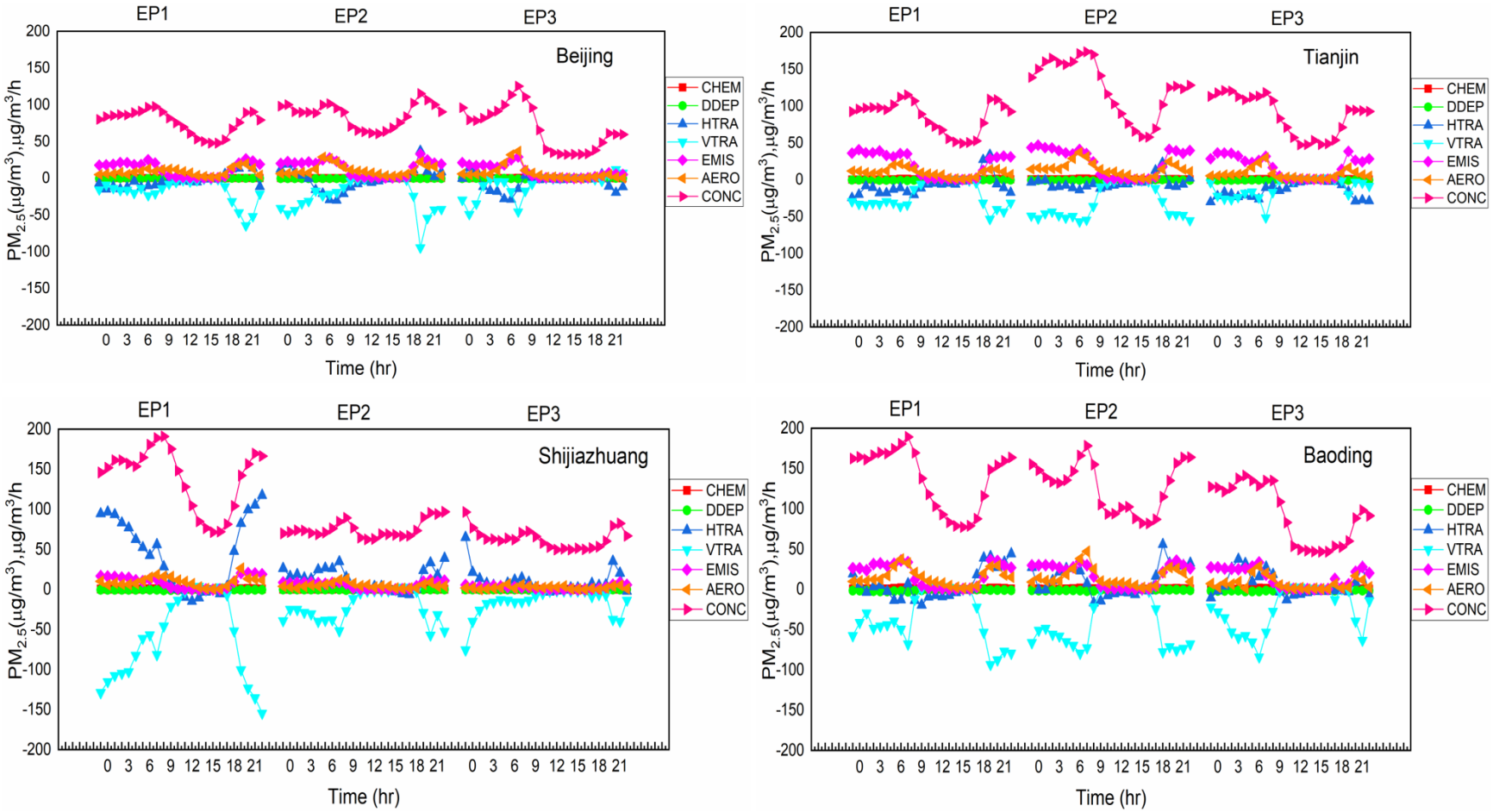

Figure S12. Diel variations of contributions of individual processes to $PM_{2.5}$ formation (Case 2) in the PBL during the three pollution episodes in the four representative cities. Abbreviations used in this figure are the same as in Fig. 1.

References

Emery, C., Tai, E., Yarwood, G. (2001). Enhanced Meteorological Modeling and Performance Evaluation for Two Texas Ozone Episodes, Prepared for the Texas Natural Resource Conservation Commission. Environ International Corporation, Novato, CA.

Sulaymon, I. D., Zhang, Y., Hopke, P. K., Hu, J., Zhang, Y., Li, L., Mei, X., Gong, K., Shi, Z., Zhao, B., Zhao, F. (2021a). Persistent high PM2.5 pollution driven by unfavorable meteorological conditions during the COVID-19 lockdown period in the Beijing-Tianjin-Hebei region, China. Environmental Research, 198. https://doi.org/10.1016/j.envres.2021.111186

Tang, L., Shang, D., Fang, X., Wu, Z., Qiu, Y., Chen, S., Li, X., Zeng, L., Guo, S., Hu, M. (2021). More significant impacts from new particle formation on haze formation during COVID-19 lockdown. *Geophysical Research Letters*, *48*, e2020GL091591. https://doi.org/10.1029/2020GL091591

Wang, P., Chen, K., Zhu, S., Wang, P., Zhang, H. (2020). Severe air pollution events not avoided by reduced anthropogenic activities during COVID-19 outbreak. Resources, Conservation and Recycling, 158. https://doi.org/10.1016/j.resconrec.2020.104814